RSC Advances

PAPER

View Article Online
View Journal | View Issue

Cite this: *RSC Adv.*, 2020, **10**, 21369

Morphology-controlled silver nanowire synthesis using a cocamidopropyl betaine-based polyol process for flexible and stretchable electronics†

Yuxiu Li, Yao Li, Zhengyang Fan, Hongwei Yang, * Ximin Yuan and Chuan Wang*

Received 7th April 2020
Accepted 20th May 2020

DOI: 10.1039/d0ra03140b

rsc.li/rsc-advances

Silver nanowire (AgNW) based transparent conductive films (TCFs) are promising building blocks for flexible and stretchable electronics to replace brittle metal oxides. Ultra-long AgNWs are preferred for enabling TCFs with excellent photoelectric properties and mechanical flexibility. Herein, a novel polyol process is proposed for the synthesis of ultra-long AgNWs, with the new finding that the addition cocamidopropyl betaine (CAB) to polyol synthesis allows the rapid production of AgNWs with an average length of ~120 μm in a high yield of ~90%. Also, a cocamidopropyl betaine assisted polyol method for the synthesis of ultra-long AgNWs is demonstrated with a possible mechanistic explanation. The prepared AgNWs are coated on a polyethylene glycol terephthalate (PET) substrate to fabricate a flexible transparent conductive film, which exhibits a low sheet resistance of ~200 Ω sq^{-1} at 88.74% transmittance with a negligible change of sheet resistance after bending. In addition, flexible TCFs based on the resulting AgNWs reveal excellent mechanical flexibility and high cyclic stability after 300 cycles of bending. The new polyol process in this work will provide a greater possibility for the practical application of long AgNWs towards flexible and wearable optoelectronic devices.

1. Introduction

Flexible electronics, as a component of very popular emerging technology in recent years, is becoming more and more an important part of the consumer electronics industry. Flexible electronic products can work normally within a certain range deformation, such as bending, folding, torsion, compression, tensile strain, *etc.* The latest developments of next-generation flexible electronics require high flexibility and transparency for both functional and aesthetic reasons,[1] especially for flexible displays,[2] wearable electronics,[3–7] electronic skin,[8–10] smart windows,[11–13] organic light-emitting diode (OLED) displays and lighting,[14–18] *etc.* Flexible circuits are the basis and core of wearable devices, and transparent conductive films (TCFs) and their structures undoubtedly play critical roles in controlling their performances.[19,20] Among various TCFs, indium tin oxide (ITO) has been widely applied in all kinds of optoelectronic devices because of its high transmittance and low sheet resistance.[21,22] Nevertheless, the finite reserves of indium and high production cost as well as that of the brittleness of ITO limit its further applications in flexible electronic devices. Hence, it is urgent to develop alternative materials of ITO to meet the needs of low-cost, flexible and wearable devices.

Up to now, the ITO alternative materials include mainly silver nanowires,[23–25] graphene,[26,27] carbon nanotube,[28,29] and metal nanowire networks,[30] *etc.* Compared with other alternative materials, AgNWs have low cost, high mechanical flexibility, and excellent optoelectronic properties, which have attracted a great deal of attention as the most promising alternatives to ITO. Thereinto, the longer length AgNWs tend to set up more sparse and effective percolation network that increases light transmission and reduces sheet resistance by offering longer percolation paths with less nanowires amount of usage, which exhibits simultaneously higher flexural resistance. Therefore, the development of ultra-long AgNWs is significant for realizing high-class flexible electronics. Unfortunately, owing to the difficulty in controlling the length of AgNWs, it is still a great challenge to realize longer AgNWs conductive networks for building flexible high-performance optoelectronic devices.

Among those methods to prepare the AgNWs, the polyol process has been considered as the most prospective method. Nevertheless, many influencing factors in this process could affect the nucleation and growth of AgNWs. Therefore, the AgNWs generated by this method has relatively short length of <100 μm.[31–35] The control of the number of seed crystals, as well as the improvement of growth process is essential to synthesize ultra-long AgNWs. Out of the above considerations, in this work, we report a novel polyol synthetic route to prepare AgNWs

State Key Laboratory of Advanced Technologies for Comprehensive Utilization of Platinum Metals, Kunming Institute of Precious Metals, 650106 Kunming, People's Republic of China. E-mail: nanolab@ipm.com.cn

† Electronic supplementary information (ESI) available. See DOI: 10.1039/d0ra03140b

with a longer length of ~120 μm. The nucleation and growth of AgNWs are efficaciously controlled by adding cocamidopropyl betaine. To the best of our knowledge, this is the first report on cocamidopropyl betaine assisted polyol process achieves the synthesis of ultra-long AgNWs. Flexible TCFs based on this AgNWs show a higher transmittance of 88.74% with a low sheet resistance of ~200 Ω sq^{-1}. In addition, a mechanical flexibility research exhibits that the sheet resistance of the AgNWs film has very little change after 300 bending cycles, which suggests good mechanical flexibility and high cyclic stability for TCFs base on ultra-long AgNWs. These results provide new design of AgNWs synthesis, and the highly transparent and mechanically stable flexible AgNWs TCFs meet the requirement for many significant applications and could play a role in the flexible electronics in a near future.

2. Experimental

2.1 Chemicals and reagents

All the chemical reagents were analytical grade and were used without further purification. Silver nitrate ($AgNO_3$, ≥99.8% of purity) was purchased from Strem Chemicals, polyvinylpyrrolidone (PVP, M_w = 1 300 000) was obtained from Sigma Aldrich. Cocamidopropyl betaine (CAB), ethylene glycol (EG, ≥99.0% of purity), and poly(vinyl alcohol) (PVA, M_w = 44.05) with 54.0–66.0 viscosity, which were purchased from Sinopharm Chemical Reagent. Ethanol (C_2H_5OH, ≥99.0% of purity) was provided by Xilong Chemical, polyethylene glycol terephthalate (PET) was furnished by Yingshang Electronic Material. Deionized (DI) water with a resistivity high than 18.2 MΩ cm generated by a purification system used throughout the experiments.

2.2 AgNWs preparation

Silver nanowires were synthesized in a solution using cocamidopropyl betaine as a novel growth addition agent. In a typical synthetic route, 3.7 g $AgNO_3$ was dissolved in 30 mL of EG at room temperature, as 'a' solution. 0.04 g cocamidopropyl betaine was dissolved in 20 mL EG at room temperature, as 'b' solution. 4.3 g PVP was added in 100 mL EG, and the solution was stirred at room temperature for about 2 h for a through dissolution, as 'c' solution. After complete dissolution, the 'b' solution and 'c' solution were added into a three-necked flask that with 850 mL of EG, and stirred at 200 r s^{-1} for 10 min. Then, the stirring rate was reduced to 80 r s^{-1}, and the 'a' solution was dropwise added with the dropping rate of 4 mL min^{-1}. After that, the stirring was stopped and the mixture solution was heated to 110 °C, and heated for 30 min at 110 °C. Afterwards, the mixture was further heated to 150 °C and kept in this temperature for 1 h 40 min to allow the growth of nanowires. Subsequently, empty the product into the mixture of DI water and ethanol, and then centrifugation at 3200 rpm for 10 min to obtain final AgNWs product. Finally, the AgNWs were dispersed in DI water for further using, and the solid content of AgNWs aqueous solution was to be 0.15%.

2.3 Ink preparation

The AgNWs ink was obtained from mixing the AgNWs and PVA solution. In brief, 0.09 g PVA was first dissolved in 30 mL of DI water form a PVA solution. Then, transfer 80 mL 0.15% AgNWs aqueous solution into centrifugal cup, and the required AgNWs was collected by centrifugal separation. Then mixed it with PVA solution and stirred for 30 min to achieve the AgNW inks with an AgNWs weight ratio of 0.4% and a PVA weight ratio of 0.3%. In this way, stable AgNWs coating ink could be obtained. This weight ratio was proved to be the most promising for the harmonious photoelectric performance of flexible film in our incipient experiments.

2.4 AgNWs films coating and curing

To make flexible transparent conductive films, polyethylene glycol terephthalate (PET) was used as the substrates of TCFs. AgNWs based TCFs were fabricated using an automatic coating machine (BEVS1811/2) at a coating speed of 50 mm s^{-1} on a PET substrate. In the typical bar-coating process, the clean bare substrate was absorbed on the platform by vacuum system, and the bar of 15 μm was fixed on the substrate (After of a significant amount of groping experimental, the coated bar of 15 μm get a suitable thick of wet film can achieve excellent photoelectric performance.). A certain amount of AgNWs ink was dropped on the PET substrate along the edge of bar. When the bar coater was turned on, AgNWs dispersion on the surface of the PET substrate form a uniform AgNWs network. After that, the as-coated wet film was annealed at 130 °C for 30 min in the atmosphere to promote wire–wire connection.

2.5 Characterization

X-ray powder diffractions (XRD) of the as-synthesized AgNWs were performed with a Rigaku D/MAX-3B X-ray powder diffractometer using Cu K_α irradiation (λ = 1.54056 Å) as an incident beam, and the spectrum was collected over the range of 2θ from 20° to 90° with a scanning step 0.02°. The structure and distribution of the as-synthesized AgNWs were measured using a FEI-Versa3D field emission scanning electron microscopy (FE-SEM), the FE-SEM images were collected by depositing the AgNWs loaded silicon wafer. UV-vis spectroscopy (PERSEE Genera TU-1901) was used to monitor the evolution of the surface resonance of the as-obtained silver nanostructures. The optical transmittance and haze of the AgNWs films were evaluated using a SGW-820 transmittance and haze analyzer. The sheet resistance of the AgNWs films was measured using a four-point probe resistivity measurement system (SB100A/2). The mechanical flexibility of the AgNWs films was determined by repeatedly bending the films. Specifically, all experiments and measurements were carried out at room temperature unless indicated otherwise.

3. Results and discussion

To characterize the chemical composition of the as-synthesized sample, the XRD patterns were studied and the results were shown in Fig. 1. Sharp peaks in the range of 20–90° (2θ) are

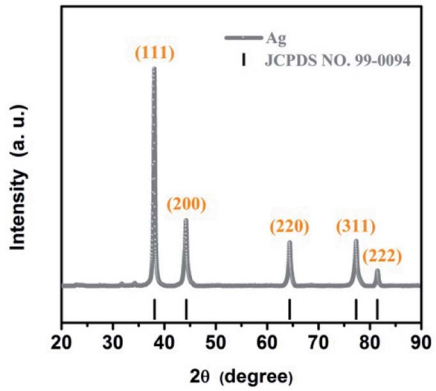

Fig. 1 XRD pattern of ultra-long AgNWs of cocamidopropyl betaine assisted synthesis.

observed from the XRD patterns, indicating that the high crystallinity of the as-synthesized AgNWs. Fig. 1 shows five typical diffraction peaks at 38.09°, 44.28°, 64.42°, 77.38°, and 81.52° assigned to the (111), (200), (220), (311), and (222) crystalline planes of the face-centered cubic (fcc) lattice, respectively, which is perfect agreement with the standard diffraction spectrum of single-crystal Ag (JCPDS no. 99-0094, space group $Fm\bar{3}m$ (225)). The lattice constant from the pattern was calculated as 4.0885 Å. This result is consistent with the standard value ($a = b = c = 4.0862$ Å). No other peaks assigned to Ag_2O are observed, proving that the as-synthesized AgNWs possess high purity and stability. Moreover, the peak at 38.09° has the highest intensity and is much sharper compared to the other four peaks, which suggests that the AgNWs have a preferential growth along the {111} direction.

To investigate the effect of cocamidopropyl betaine in AgNWs synthesis process, the preparation without cocamidopropyl betaine was performed, and shown in Fig. S1.† And we can see from Fig. S1(a),† the as-synthesized sample is composed of a large proportion of the nanoparticles and a fraction of the nanorods. The more detail structural features of the sample based on polyol method without cocamidopropyl betaine were shown in Fig. S1(b).† It can be noticed that the diameter of nanoparticles in a range from 172 nm to 280 nm, and the diameter of nanorods about to be 150 nm. The controlled trial results suggest that the AgNWs would not realization without the participation of the cocamidopropyl betaine.

In order to further prove the contribution of cocamidopropyl betaine to nanowires growth. The microstructure and morphology information of the sample under the participation of the cocamidopropyl betaine were analyzed, and the corresponding FE-SEM images were presented in Fig. 2. The FE-SEM images of the as-synthesized sample from different location under different resolution shows a typical wire like structure. Fig. 2(a) and (b) show FE-SEM images at low magnification and confirm the longer, high yield, and particle-free silver nanowires. As can be seen from the figures, the average length of AgNWs is measured to be about ~120 μm by random selecting hundreds of nanowires, the length in a range from 115 μm to

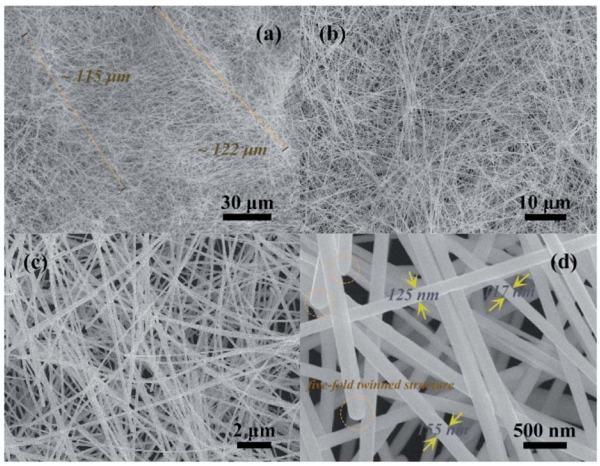

Fig. 2 (a) and (b) show low resolution FE-SEM images of ultra-long AgNWs of cocamidopropyl betaine assisted synthesis. (c) and (d) corresponding to the high resolution FE-SEM images.

122 μm, which indicates AgNWs possess high uniformity. To probe the detailed morphology of AgNWs, Fig. 2(c) and (d) reveal the larger magnified images of AgNWs, and exhibit a comparatively smooth surface. It can be seen from the figures that the diameter of AgNWs varies from 117 nm up to 155 nm with a narrow size distribution, and the average diameter is about ~130 nm. And, more remarkable, a special part is marked by the brown circles, the ends of the nanowires show a rounded and pyramidal profile what could be called "five-fold twinned structure". It means that the silver nanowires have five straight side edges parallel to the longitudinal axis.[36]

Composition analysis was examined using EDX as for ultra-long AgNWs, as indicated in Fig. S2.† Clearly, Si, Ag, Pt, Ni, C and O elements were detected. It is worthwhile to note that the Si element is found with a higher content. The Si element comes from the silicon wafer, which is used as a support of the AgNWs, while Pt and Ni are the impurities from silicon wafer, and the C and O derive from the air. Therefore, the existence of the Ag with a content of 32.04 wt%, which indicates the product are a high purity AgNWs.

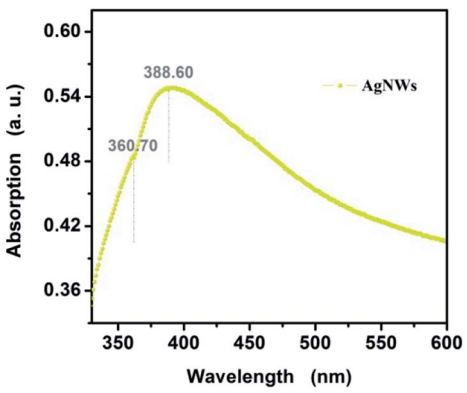

Fig. 3 UV-vis absorption spectra of ultra-long AgNWs of cocamidopropyl betaine assisted synthesis.

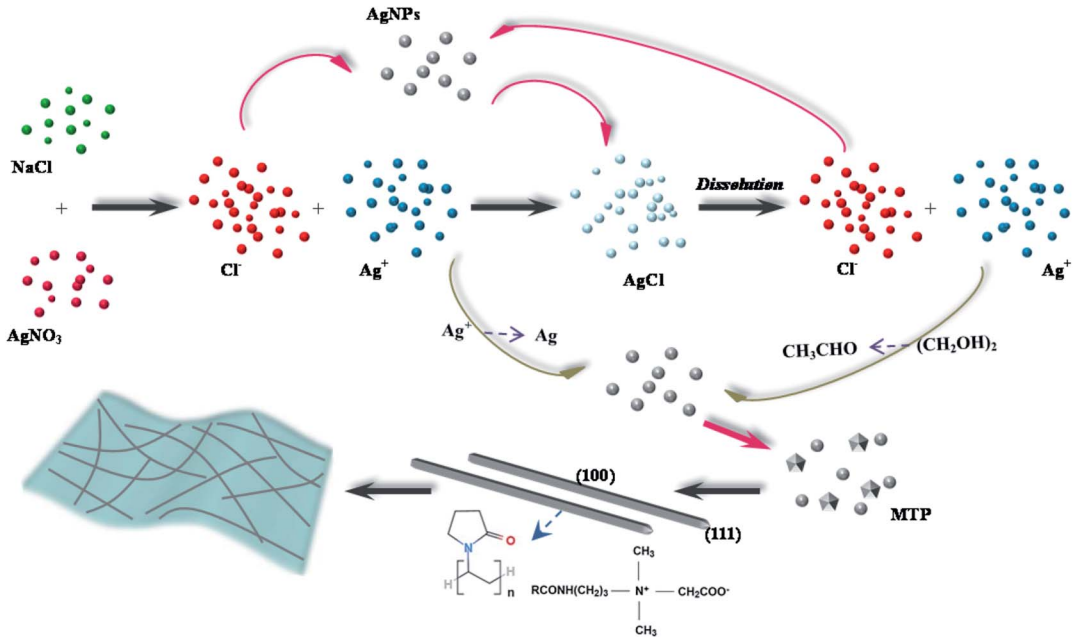

Fig. 4 Schematic illustration of the proposed formation process of the ultra-long AgNWs.

Optical absorption characterization could also provide key clues to the morphology of the AgNWs. Fig. 3 exhibits the UV-vis spectrum of AgNWs dispersed in aqueous solution with a standard UV-vis spectrum of pure AgNWs, which shows the most prominent characteristic of silver nanowires. That is, one sharp peak at 388.60 nm and a slight shoulder at 360.70 nm, which ascribes to the localized surface plasmon resonances and the influence of the pentagonal cross-section of the nanowires, as other studies in the literature have reported.[37] In addition, the spectrum red shift and the wide narrow bandwidth suggest the slightly larger diameter for cocamidopropyl betaine-assisted AgNWs. More optimistically, no other absorption peaks between 400–450 nm correspond to silver nanoparticles in the raw sample. This observation indicates that the AgNWs possess high purity, which is in good agreement with the result observed in SEM.

For polyol process, it has been demonstrated that the surfactant has a capping function for {100} facets, it provides an effective opportunity to control the type of seeds.[38] In order to provide a more powerful capping function and improve the yield of five-fold multiple twinned seeds, we designed a cocamidopropyl betaine-based polyol process to synthesize ultra-long AgNWs in this article, as schematically illustrated in Fig. 4. The cocamidopropyl betaine has play a role in both the end-capping and structure inducing, also enhance the rate of reaction. It is known that the cocamidopropyl betaine with less than 7% NaCl can be obtained by quaternarization. The Cl^- not only can react with Ag^+, but also can be combined with silver nanoparticles (AgNPs) of new nucleation to produce AgCl, and the AgCl will dissolve in EG solution at high temperatures to form new active Cl^- continue to react with AgNPs. The Cl^- as an intermediate can accelerate the AgNPs crystal nucleation.[39] Meanwhile, $(CH_2OH)_2$ can be resolved into CH_3CHO with the increase of reaction temperature, the Ag^+ is deoxidized into Ag atom through CH_3CHO. On the other hand, the adsorption of (100) facets of AgNPs to PVP is stronger than (111) facets due to the activity of AgNPs (111) facets is lower than that the (100) facets.[40] It can thus effectively inhibit the AgNPs growing on the (100) facets, so the AgNPs grow continually in (111) facets along with the ⟨100⟩ direction. Additionally, there are strong adsorption function between Ag atoms of (100) facets and N atoms from cocamidopropyl betaine, further limiting their lateral growth,[41] which provide more opportunities to produce five-fold multiple twinned particles, and to further grown into long AgNWs.

To formulate the AgNWs ink for bar coating, these properties should be optimized, including stabilization of AgNWs in the ink, wetting, spreading, drying of the coated AgNWs films, which are pivotal to the fabrication of high transparency and uniform AgNWs films. In this study, the ink was prepared by adding AgNWs to a poly(vinyl alcohol) solution with DI water. As well known, the DI water possesses high surface tension, which

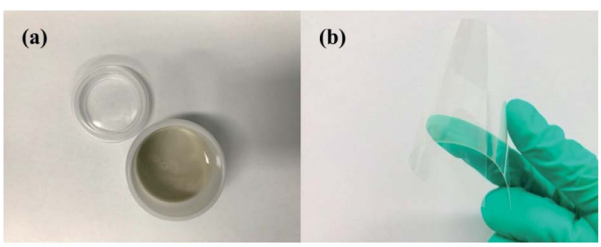

Fig. 5 Typical photo-diagrams of (a) AgNWs conductive ink and (b) flexible TCFs based on the ultra-long AgNWs.

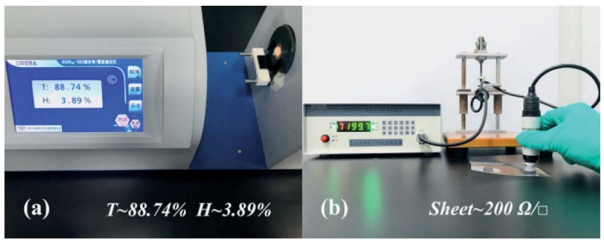

Fig. 6 Optoelectronic performances of flexible TCFs based on the ultra-long AgNWs including (a) transmittance and haze, and (b) sheet resistance.

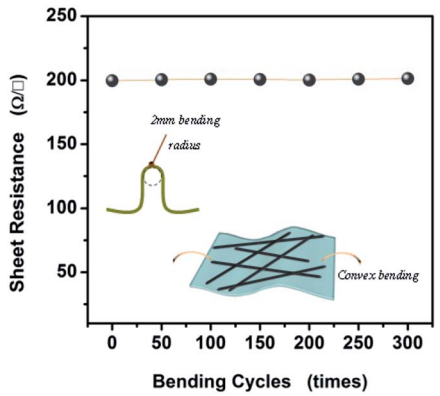

Fig. 7 Sheet resistances of flexible TCFs based on the ultra-long AgNWs under 300 bending cycles with a bending radius of 2.0 mm.

will tend to result in aggregation of AgNWs and shrinkage of films. The addition of poly(vinyl alcohol) not only plays the role of adhesive, but also can decrease surface tension of water because of its surface activity. As shown in Fig. 5(a), the AgNWs ink has the offwhite appearance, which should be attributed to the long length of silver nanowires. The as-coated AgNWs film, as shown in Fig. 5(b), exhibits excellent flexibility and high optical transparency.

To more specifically exam the optoelectronic performances of the as-fabricated AgNWs film, the transmittance and haze of AgNWs film was measured, as shown in Fig. 6. The AgNWs film has a high transmittance of 88.74%, a haze of 3.89% and a sheet resistance of ~200 Ω sq^{-1}, which is potential for application in some flexible devices.[42]

The flexibility and reliability of the AgNWs film were further evaluated by bending experiments, which are of importance relevance of their potential applications in wearable electronics. The changes of sheet resistance with bending cycles were investigated with a bending radius of 2.0 mm for 300 cycles, and shown in Fig. 7. Although the bending radius is just 2.0 mm, the sheet resistance of the as-fabricated AgNWs film maintains nearly at a constant value during the bending test. The measurement of resistance change is approximately 0.55 Ω sq^{-1} to 1.61 Ω sq^{-1}, regardless of cycle number, suggesting that the AgNWs film has remarkable flexibility and reliability, critical for many wearable device applications.

4. Conclusions

In summary, we have presented a novel high-yield method for the synthesis of ultra-long AgNWs with a length of ~120 μm. The nucleation and growth processes of AgNWs can be effectively controlled by the adding of cocamidopropyl betaine and the synergy of poly-vinylpyrrolidone. Flexible TCFs based on the ultra-long AgNWs exhibit low sheet resistance of ~200 Ω sq^{-1} at 88.74% transmittance, good mechanical flexibility and high cyclic stability with a negligible change of sheet resistance after bending, thus providing a new opportunity for the synthesis of ultra-long silver nanowires and a potential application in the field of flexible nano-optoelectronics.

Conflicts of interest

There are no conflicts to declare.

Acknowledgements

This work was supported by National Natural Science Foundation of China (Grant No. 21761016), Young and Middle-aged Academic and Technical Leaders Reserve Talents Program of Yunnan Province (Grant No. 2017HB060), Applied Basic Research Foundation of Yunnan Province (Grant No. 2017FB142), and Major R&D Project of Yunnan Province (Grant No. 2018ZE001).

References

1 X. Liu, D. D. Li, X. Chen, W. Y. Lai and W. Huang, *ACS Appl. Mater. Interfaces*, 2018, **10**, 32536–32542.
2 R. Manda, S. Pagidi, Y. J. Lim, R. He, S. M. Song, J. H. Lee, G. D. Lee and S. H. Lee, *J. Mol. Liq.*, 2019, 111314.
3 X. D. Wang, Y. F. Zhang, X. J. Zhang, Z. H. Huo, X. Y. Li, M. L. Que, Z. C. Peng, H. Wang and C. F. Pan, *Adv. Mater.*, 2018, **30**, 1706738.
4 L. Li, Z. Luo, D. Chen, K. Jiang, W. Han and G. Z. Shen, *Small*, 2018, **14**, 1702829.
5 C. Y. Wang, K. L. Xia, H. M. Wang, X. P. Liang, Z. Yin and Y. Y. Zhang, *Adv. Mater.*, 2019, **31**, 1801072.
6 M. X. Xu, J. J. Qi, F. Li and Y. Zhang, *Nanoscale*, 2018, **10**, 5264–5271.
7 P. Xiang, X. F. Chen, B. B. Xiao and Z. M. Wang, *ACS Appl. Mater. Interfaces*, 2019, **11**, 8115–8125.
8 L. Nela, J. S. Tang, Q. Cao, G. Tulevski and S. J. Han, *Nano Lett.*, 2018, **18**, 2054–2059.
9 F. X. Yin, J. Z. Yang, H. F. Peng and W. J. Yuan, *J. Mater. Chem. C*, 2018, **6**, 6840–6846.
10 M. Li, Y. M. Wang, Y. Zhang, H. M. Zhou, Z. G. Huang and D. Q. Li, *J. Mater. Chem. C*, 2018, **6**, 5877–5887.
11 D. J. Kim, D. Y. Hwang, J. Y. Park and H. K. Kim, *J. Alloys Compd.*, 2018, **765**, 1090–1098.
12 S. M. Lee, J. Y. Park and H. K. Kim, *Adv. Mater. Interfaces*, 2018, **5**, 1801082.
13 H. J. Seo, Y. C. Nah and H. K. Kim, *RSC Adv.*, 2018, **8**, 26968–26977.

14 I. J. Park, T. I. Kim, T. Yoon, S. Kang, H. Cho, N. S. Cho, J. I. Lee, T. S. Kim and S. Y. Choi, *Adv. Funct. Mater.*, 2018, **28**, 1704435.
15 M. Z. Wei, H. Wang, J. T. Wang, P. Chen, W. Z. Zhao, X. Y. Chen, J. H. Guo, B. Kang and Y. Duan, *Org. Electron.*, 2018, **63**, 71–77.
16 J. Y. Tseng, L. Lee, Y. C. Huang, J. H. Chang, T. Y. Su, Y. C. Shih, H. W. Lin and Y. L. Chueh, *Small*, 2018, **14**, 1800541.
17 R. E. Triambulo, J. H. Kim and J. W. Park, *Org. Electron.*, 2019, **71**, 220–226.
18 H. Sim, C. Kim, S. Bok, M. K. Kim, H. Oh, G. H. Lim, S. M. Cho and B. Lim, *Nanoscale*, 2018, **10**, 12087–12092.
19 F. X. Wang, X. W. Wu, X. H. Yuan, Z. C. Liu, Y. Zhang, L. J. Fu, Y. S. Zhu, Q. M. Zhou, Y. P. Wu and W. Huang, *Chem. Soc. Rev.*, 2017, **46**, 6816–6854.
20 Y. G. Wang, Y. F. Song and Y. Y. Xia, *Chem. Soc. Rev.*, 2016, **45**, 5925–5950.
21 L. Zhou, M. J. Yu, X. L. Chen, S. H. Nie, W. Y. Lai, W. M. Su, Z. Cui and W. Huang, *Adv. Funct. Mater.*, 2018, **28**, 1705955.
22 S. I. Lee, G. J. Yun, J. W. Kim, G. Hanta, K. Y. Liang, L. Kojvic, L. S. Hui, A. Turak and W. Y. Kim, *Sci. Rep.*, 2019, **9**, 2411.
23 Z. Cui, Y. W. Han, Q. J. Huang, J. Y. Dong and Y. Zhu, *Nanoscale*, 2018, **10**, 6806–6811.
24 J. Sun, W. H. Zhou, H. B. Yang, X. Zhen, L. F. Ma, D. Williams, X. D. Sun and M. F. Lang, *Chem. Commun.*, 2018, **54**, 4923–4926.
25 J. J. Chen, S. L. Liu, H. B. Wu, E. Sowade, R. R. Baumann, Y. Wang, F. Q. Gu, C. R. L. Liu and Z. S. Feng, *Mater. Des.*, 2018, **154**, 266–274.
26 D. H. Song, E. B. Secor, Y. Wang, M. C. Hersam and C. D. Frisbie, *ACS Appl. Mater. Interfaces*, 2018, **10**, 22303–22310.
27 T. S. Tran, N. K. Dutta and N. R. Choudhury, *Adv. Colloid Interface Sci.*, 2018, **261**, 41–61.
28 R. Fischer, A. Gregori, S. Sahakalkan, D. Hartmann, P. Buchele, S. F. Tedde and O. Schmidt, *Org. Electron.*, 2018, **62**, 351–356.
29 Y. Y. Chen, Y. Sun, Q. B. Zhu, B. W. Wang, X. Yan, S. Qiu, Q. W. Li, P. X. Hou, C. Liu, D. M. Sun and H. M. Cheng, *Adv. Sci.*, 2018, **5**, 1700965.
30 I. Hong, S. Lee, D. Kim, H. Cho, Y. Roh, H. An, S. Hong, S. H. Ko and S. Han, *Nanotechnology*, 2018, **30**, 074001.
31 H. Yang, T. R. Chen, H. F. Wang, S. C. Bai and X. Z. Guo, *Mater. Res. Bull.*, 2018, **102**, 79–85.
32 B. W. Lei, J. Wang, Y. G. Du and K. L. Zhang, *Mater. Res. Express*, 2017, **4**, 075052.
33 E. J. Lee, Y. H. Kim, D. K. Hwang, W. K. Choi and J. Y. Kim, *RSC Adv.*, 2016, **6**, 11702–11710.
34 T. N. Trung, V. K. Arepalli, R. Gudala and E. T. Kim, *Mater. Lett.*, 2017, **194**, 66–69.
35 Y. Wei, Q. L. Zhang, H. J. Wan, Y. N. Zhang, S. W. Zheng and Y. Zhang, *Phys. Chem. Chem. Phys.*, 2018, **20**, 18837–18843.
36 T. R. Chen, H. F. Wang, H. Yang, S. C. Bai and X. Z. Guo, *Mater. Res. Express*, 2018, **5**, 066426.
37 M. Rothe, Y. H. Zhao, G. Kewes, Z. Kochovski, W. Sigle, P. A. Aken, C. Koch, M. Ballauff, Y. Lu and O. Benson, *Sci. Rep.*, 2019, **9**, 3859.
38 R. R. Da Silva, M. X. Yang, S. I. Choi, M. F. Chi, M. Luo, C. L. Zhang, Z. Y. Li, P. Hc Camargo, S. Jl Ribeiro and Y. N. Xia, *ACS Nano*, 2016, **10**, 7892–7900.
39 M. Tsuji, K. Matsumoto, P. Jiang, R. Matsuo, X. L. Tang and K. S. N. Kamarudin, *Colloids Surf., A*, 2008, **316**, 266–277.
40 N. Murshid and V. Kitaev, *Chem. Commun.*, 2014, **50**, 1247–1249.
41 J. Xu, W. J. Liu, H. L. Liu and Y. Hu, *Front. Chem. Eng. China*, 2007, **1**, 221–227.
42 W. Zhao, S. S. Wang, H. T. Cao, L. H. Xie, C. S. Hong, L. Z. Jin, M. N. Yu, H. Zhang, Z. Y. Zhang, L. H. Huang and W. Huang, *RSC Adv.*, 2019, **9**, 1933–1938.